https://doi.org/10.1016/j.apenergy.2021.117875

Comparative study of the dynamic programming-based and rule-based operation strategies for grid-connected PV-battery systems of office buildings

Bin Zou[a, b], Jinqing Peng [a, b *], Sihui Li [a, b], Yi Li [a, b], Jinyue Yan [c], Hongxing Yang [d]

[a] College of Civil Engineering, Hunan University, Changsha 410082, Hunan, China

[b] Key Laboratory of Building Safety and Energy Efficiency of Ministry of Education, Hunan University, Changsha, Hunan, China.

[c] Mälardalen University, Future Energy Center, Stockholm, Sweden.

[d] Renewable Energy Research Group (RERG), Department of Building Services Engineering, The Hong Kong Polytechnic University, Kowloon, Hong Kong, China.vg

Abstract

The proper operation strategy is of great importance for photovoltaic-battery (PVB) systems to achieve desirable performance. Therefore, it's necessary to identify and evaluate the characteristics of different operation strategies for engineering application. In this study, three operation strategies including the dynamic programming (DP)-based strategy and two widely used rule-based strategies, namely the maximizing self-consumption (MSC) strategy and time-of-use (TOU) strategy, are compared comprehensively for the grid-connected PVB system of an office building. Several important performance aspects, including battery charge/discharge process, techno-

economic performance, energy distribution, battery aging and impacts on utility grid, are analyzed and compared. The results show that the DP strategy has greater flexibility than the rule-based strategies to adapt to different PV-load distributions and electricity pricing mechanisms, and has the advantage of achieving better economic performance and reducing burden on the grid. Although the economic performance of the MSC strategy is relatively poor, it has the highest self-consumption rate (*SCR*) and self-sufficiency rate (*SSR*), thereby having the advantage of using PV generation in timely manner to suit load demand. In addition, the MSC strategy results in the least battery aging, while having the greatest negative impact on the utility grid. The TOU strategy only outperforms the MSC strategy in economic performance under the condition of relatively low battery cost (<1600 CNY/kWh) and causes the most battery aging as well. The findings in this work can provide guidance for decisionmakers to determine the proper management strategy for practical grid-connected PVB systems.

Keywords: photovoltaic-battery (PVB) system; operation strategies; comparative study; dynamic programming (DP); maximizing self-consumption (MSC); time-of-use (TOU)

* Corresponding author: College of Civil Engineering, Hunan University, Changsha 410082, Hunan, China.

E-mail: jallenpeng@gmail.com (Jinqing Peng)

Nomenclature

C	cost (CNY)
E	total energy (kWh)
E_b	battery rated capacity (kWh)
G	global solar radiation intensity on the horizontal plane (W/m^2)
G_b	beam solar radiation intensity on the horizontal plane (W/m^2)
G_d	diffuse solar radiation intensity on the horizontal plane (W/m^2)
G_T	solar radiation intensity incident on PV array (W/m^2)
I_L	photocurrent (A)
I_o	diode reverse saturation current (A)
I_{pv}	PV current (A)
k	Boltzmann constant (J/K)
L_{cyc}	life cycle number of the battery
$N_{b,dis}$	total discharge hours of the battery
P	power (kW)
q	electron charge constant
R_b	ratio of direct radiation of inclined plane
R_s	PV module series resistance (Ω)
T_c	PV module temperature (°C)
T / t	Time (h)
V_{pv}	PV voltage (V)
x_b	unit capacity cost of the battery (CNY/kWh)
x_{inv}	initial investment per unit capacity of the battery (CNY/kWh)
x_{mai}	maintenance cost per unit capacity of the battery (CNY/kWh)
x_{pv}	average cost of PV power generation (CNY/kWh)

Greek symbols

α	installation tilt angle (°)
β_{cal}	battery calendar aging
β_{cyc}	battery cycle aging
β_{toal}	total battery aging
γ	PV curve-fitting parameter
ε	binary number (0 or 1)
η	efficiency (%)
ρ	reflectance of the ground
Δt	time step

Subscripts

b	battery
ch	charge
d / *de*	load demand
dis	discharge
ex	export
g	grid
im	import
max	maximum
min	minimum
p / *pv*	photovoltaic
ref	reference value
total	total value
b-d / *b-g*	energy flow from battery to load / grid
g-b / *g-d*	energy flow from grid to battery / load
p-b / *p-d* / *p-g*	energy flow from PV to battery / load / grid

Abbreviations

DP	dynamic programming

ERP	electricity retail price
FiT	feed-in-tariff
LCR	load coverage ratio
LP	linear programming
MSC	maximizing self-consumption
MILP	mixed integer linear programming
MPPT	maximum power point tracking
PV	photovoltaic
PVB	photovoltaic-battery
SCR	self-consumption rate
SOC	state of charge
SOH	state of health
SSR	self-sufficiency rate
TOU	time-of-use
ZEB	zero energy building

1. Introduction

A growing concern has been paid to building sector due to its rapid increasing energy consumption and the negative environmental effects [1]. As one of the biggest energy consumers, the building sector accounts for about 40% of the total energy consumption and more than 30% of total CO_2 emissions worldwide [2, 3], which calls for the need of technology innovations [4], efficiency improvement and sustainability development of buildings [5]. In recent decades, the concept of zero energy buildings (ZEB) has widely been accepted [6], and implemented with the application of various

energy-efficiency measures including renewable energy technologies [7]. Driven by global energy and environmental issues, and the requirement of sustainable development, renewable energy grew almost three times faster than fossil fuels and nuclear energy in the past five years [8], among which solar energy is the most developed and used one. Due to the outstanding advantage of low cost [9], eco-friendliness, and easy integration with buildings [10, 11], solar photovoltaics (PV) has been the most commonly used renewable energy technology in the building sector [12]. However, since PV output is highly affected by weather conditions, it has the shortcoming of intermittence and instability. As a result, batteries are usually adopted to store surplus PV generation to increase the PV self-sufficiency [13] and self-consumption [14]. Since the charge and discharge of the battery can be controlled flexibly, the PV-battery (PVB) system improves greatly the energy regulation initiative of end consumers who can manage the energy flow actively based on certain operation strategies [15]. In this context, a proper operation strategy is of great importance to achieving the desirable performance of PVB systems [16].

Plenty of studies have been conducted to explore appropriate operation strategies for PVB systems based on different objectives [15]. The strategy that aims at maximizing self-consumption (MSC) of the PV generation is one of the most commonly used operation strategies for PVB systems, especially for distributed PV systems [17]. The MSC strategy is a simple energy management strategy that tries to consume the PV generation with the maximum allowable rate as timely and completely

as possible [15]. Braun et al. [18] analyzed the effects of batteries on self-consumption, and concluded that proper deployment of batteries increased greatly the local consumption of PV generation. Based on the purpose of maximizing the PV self-consumption and reducing the energy exported to the grid, some researchers explored the optimization approach for PV size [19] or energy storage capacity [20]. Luthander et al. [21] conducted a detailed review of existing research on PV self-consumption in buildings, and found that the relative self-consumption could be improved by 13-24% with collocating battery size properly. Sharma et al. [22] performed an optimization of the size of batteries for a typical net zero energy home with rooftop PV in South Australia based on the MSC operation strategy. According to Ref. [23], the self-consumption rate (*SCR*) could be increased by 20-50% with proper batteries installed. Zhang et al. [17] performed a detailed techno-economic analysis of a grid-connected household PVB system under the condition of MSC operation strategy. The MSC strategy was also used together with the limit of the state of charge (*SOC*) of batteries to reduce battery degradation [24]. In that study, the maximum limit of the *SOC* of the battery was set as a constraint condition to ensure battery safety. It is expected that the MSC strategy will be more popular with the continuous decrease of financial subsidies, especially for distributed systems. It can be found from above literature survey that the MSC operation strategy has been widely used for both capacity optimization and performance assessment of the PVB system. However, researchers usually focused on the superiority of the MSC strategy in maximizing the *SCR* of PV generation, while

seldom evaluated comprehensively other aspects of the strategy, such as economic performance, energy flow distribution, battery aging and impacts on utility grid.

In order to promote the application of PVB systems and incentivize demand-side participation in energy management, the feed-in-tariff (FiT) and the time-of-use (TOU) tariff were introduced in many countries [25]. Some researchers explored the design of TOU tariff mechanism [26, 27]. In Ref. [26] the optimization approach for designing the TOU rate was discussed, and Ref. [27] designed the TOU tariff using Gaussian Mixture Model. As a result, achieving economic benefit through the FiT and the electricity price difference between the peak-valley periods has become another important goal for prosumers [28], which is called the TOU strategy. Gitizadeh et al. [29] and Hassan et al. [30] conducted the battery capacity optimization based on tariff incentives. Ratnam et al. [31] revealed that the majority of customers with PVB systems made annual savings when provided with FiTs. Zhang et al. [32] conducted an optimization study on scheduling the residential PVB systems under the conditions of both TOU tariff and step tariff. In the study of Liu et al. [33], both single-criterion and multi-criterion optimizations were performed by comprehensively considering technical, economic and environmental performances of the PVB system with the TOU strategy adopted. In that study, the energy limit exported to the grid was also considered to reduce the negative effects on the grid. In their following study [34], experiments on a PVB system under the MSC strategy and the TOU strategy were carried out to explore the system performance and validate the energy management models developed for

simulation of hybrid renewable energy systems in a typical high-rise building in Hong Kong. The TOU operation strategy also has relatively simple control rules which involve charging the battery with the utility grid during valley price periods, ready for discharge in peak price periods for load demand, aiming at achieving economic benefit. Therefore, the TOU operation strategy was also widely used and accepted by both researchers and consumers. However, characterized by the economic advantage, the TOU operation strategy was usually treated partially with rare discussion on other aspects of performance, and seldom compared with other operation strategies.

Both MSC strategy and TOU strategy are rule-based strategies, which have great practicability, and have therefore been used widely in engineering practice. However, limited by the their own “rules”, these two strategies cannot realize some operation requirements of the consumers. Therefore, some optimization methods have also been used for determining the suitable energy management strategy for PVB systems [15, 35]. Heuristic methods, especially the genetic algorithm (GA) and the particle swarm optimization (PSO), were usually used for optimal design of renewable systems [35]. Ghorbani et al. [36] adopted a GA-PSO and multi-objective PSO (MOPSO) method to optimize an off-grid battery-wind-battery system based on the purpose of achieving the lowest total present cost and loss of power supply probability. Some researchers adopted GA or PSO to solve the optimization problems for hybrid distributed energy systems which involved PV panels, wind turbines [37], heating and cooling systems [38], energy storage [39], and biomass energy [40]. GA and PSO are mainly used for

optimal sizing or placement of distributed energy systems [35], whereas are very difficult to be used for optimization of the dynamic operation process of energy systems. Moreover, when used for a relatively complex system, those methods are time-consuming, and susceptible to converging in the local optima. Instead, mathematical programming methods, such as the linear programming (LP) and the dynamic programming (DP), are usually used for optimization of scheduling of energy systems [15, 35]. Nottrot et al. [41] optimized the battery dispatch of a PV grid-connected system using the LP algorithm for minimizing the net-peak load. Georgiou et al. [42] used the LP algorithm to optimize the energy storage schedule of a battery in a PV grid-connected system for nearly zero energy buildings. Yang et al. [43] conducted techno-economic and environmental optimization of a household PVB system using the mixed integer linear programming (MILP) method. Javadi et al. [44] adopted a stochastic MILP method to model the self-scheduling problem of a household PVB system, and discussed the effects of different demand response programs on utilizing the system for best results. The LP is an effective method to optimize the scheduling of PVB systems, especially in a short time period such as several hours or one day. When used for complex systems or solving large time scale optimization problems, such as more than one year or the whole lifetime period, a large number of decision variables are needed for LP, which leads to a complicated solving process and requires very long computing time. In addition, the LP can only be used for linear problems, which limits its application. As a result, another useful mathematic programming method, the dynamic

programming (DP) method, which has attracted much attention for optimizing management of renewable energy systems in recent years [45, 46]. Chen et al. [45] used the DP method to optimize the operation of a combined heat and power system, and Bahlawan et al. [46] used the method for optimization of the sizing and operation of a hybrid energy plant. Bernasconi et al. [47] adopted the DP algorithm to determine the optimal cash flow for a residential PVB system, and confirmed the meaningful economic benefit of the proposed prediction method. In Ref. [48], the DP method was used to decide the state of charge (*SOC*) schedule of the battery to find the trade-off between consumer energy cost and battery health. Ming et al [49] carried out a daily optimal generation scheduling of a hydro-PV plant to meet the load demand and minimize water consumption. Mahmoudimehr et al. [50] developed a novel multi-objective DP method for performance management of a solar thermal power plant. The DP algorithm is a powerful tool for solving multistage optimization problems, where the decision is made from a decision set based on the adopted optimization criteria [51]. This is an effective method to make a series of interrelated decisions in an optimal way for a dynamic system [51]. Every step in which the DP method solve the problem just need to find the optimal value at the current step, which makes the solving process much simple. Compared with other optimization methods, including GA, PSO and LP (or MILP), the DP method has several obvious advantages: (1) DP is suitable for both linear and nonlinear problems; (2) DP can achieve the global optimum; (3) when used for complex systems or solving large time scale optimization problems, DP has a much

shorter computing time. Therefore, the operation strategy of PVB system that is based on the DP method will also be discussed in this study. The features of the DP-based strategy will be identified clearly and assessed comprehensively.

From the literature review above, it is found that various operation strategies have been proposed based on different algorithms and objectives for PVB systems. A comparison of operation strategies in terms of different performance achievements is crucial to determine the best energy management scheme in engineering practice. There are several researchers who have compared the performance of different strategies. Zhang et al. [52] introduced three strategies, including the MSC strategy, the dynamic price load shifting strategy, and the hybrid operation strategy, to assess the grid-connected PVB system in terms of self-sufficiency rate (*SSR*) and net present value (*NPV*). In that study, the dynamic price load shifting strategy is similar to the TOU strategy, which charges the battery at low price and discharge at high price. The electricity price changed every day and was determined 24 h ahead. The hybrid strategy combined the MSC strategy and the dynamic price load shifting strategy together. It was found that the MSC strategy and the dynamic price load shifting strategy had a similar performance as the electricity price was not large enough, and the hybrid operation strategy was the best for achieving desirable performance. Angenendt et al. [24] compared two forecast-based operation strategies and the MSC strategy with *SOC* limit and exported energy cut-off limit. In that study, the *SOC* limit and the exported energy cut-off limit were set to reduce battery degradation and grid burden. Two

forecast strategies including the perfect forecast and the persistence forecast, were adopted to analyze the effects of energy prediction on operation performance. It was indicated that the forecast-based strategies can increase the battery lifetime and reduce the operation cost by up to 12%. Mulleriyawage et al. [53] developed an economic optimization strategy based on the FiT for a residential battery storage system, and compared the strategy with the MSC strategy. It was stated that the developed strategy outperformed the MSC strategy in terms of both total cost and PV curtailment avoidance.

In previous studies, researchers focused on finding strategies to solve problems in their discussed situations, and highlighted the advantages of the proposed strategies. Only one or two characteristics, especially the technical and economic performance, are generally discussed in previous research, which sometimes leads to narrower conclusions. Other performance aspects such as energy distribution, battery degradation and impacts on the grid were seldom analyzed in those studies, consequently rarely achieving overall assessment of each strategy. Moreover, all of the past comparative studies of strategies are conducted for residential buildings. As a matter of fact, due to the great timing alignment between PV generation and the load demand of office buildings, PVB systems are also particularly suited for application in office buildings. In this study, three operation strategies which can be widely used for any PVB systems, including the DP-based strategy and two rule-based strategies, namely the MSC strategy and the TOU strategy, will be discussed and compared comprehensively in

terms of the annual performance used in office buildings. The comparisons are made considering several important aspects of performance, which include battery charge/discharge performance, techno-economic performance, energy flow distribution, battery aging and impacts on the utility grid, aiming at achieving an overall and comprehensive assessment of each strategy. The findings of this study are intended to provide a guidance for decisionmakers to determine the most suitable operation strategy for PVB systems in engineering practice.

2. Methodology

2.1 System configuration

As shown in Fig. 1, the grid-connected PVB system is mainly composed of PV array, energy storage system (battery bank), utility grid, building (load), DC/AC inverter, MPPT controller and charge/discharge controller. The MPPT controller is the maximum power point tracking controller which ensures the maximum PV output. The PV generated electricity can flow to the load, the battery, or the grid according to the specific requirement. The charge/discharge controller regulates the charge and discharge process of the battery. The utility grid can supply electricity to the load and the battery bank, and receive electricity from the PV array and battery bank as needed. It is worth noting that in this study, there is no limit to the power that can be exported to the utility grid.

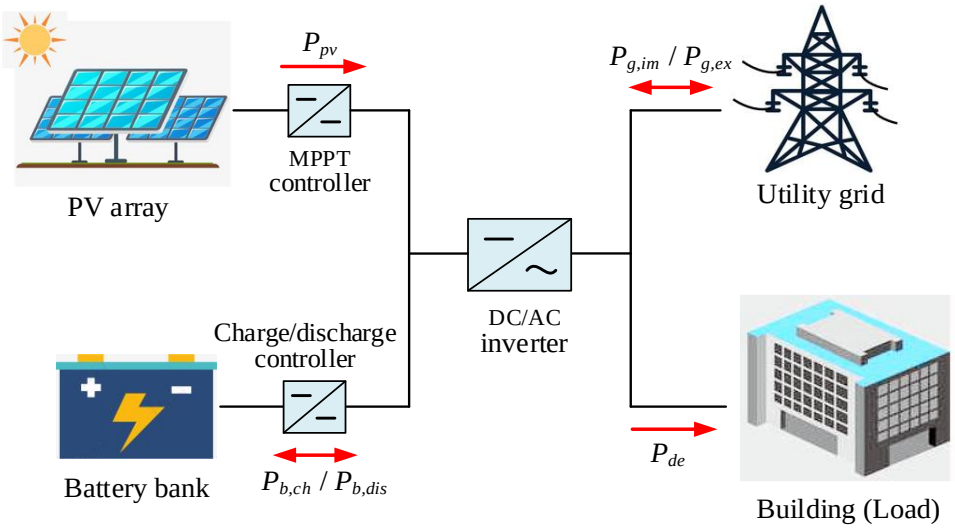

Fig. 1 Schematic of the grid-connected PVB system

2.2 Modelling and performance indicators

2.2.1 Building load

In this study, a typical 3-floor office building in Changsha, a typical city in the hot-summer and cold-winter area in China, was selected as the target building. The geometric model of the building was established in SketchUp, as shown in Fig. 2, and then imported into EnergyPlus for simulation. The dimension of the building is 49.9 m (length) × 33.3 m (width) × 12 m (height). The thermal parameters of building envelopes were determined based on "Design Standard for Energy Efficiency of Public Buildings" (GB50189-2015), as given in Table 1. The occupied area per person and the equipment heat loss per unit area (including lighting and office facilities) were set as 12 m^2/person and 20 W/m^2, respectively. The schedules of indoor occupants and office equipment in each day are given in Table 2. The weather data of the typical meteorological year of Changsha were used for building energy simulation.

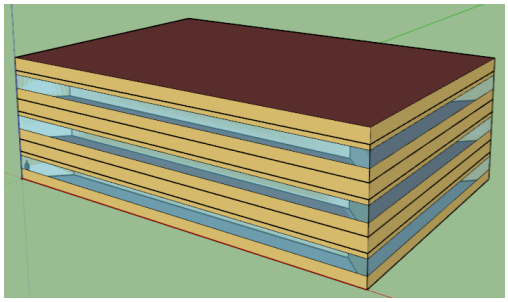

Fig. 2 Building model (middle office building)

Table 1 Thermal parameters of the building envelopes

Parameters	Thermal resistance (m^2•K/W)
External wall	1.95
Roof	2.52
Floor	1.53
Window	0.47

Table 2 Schedule of occupants and equipment

Time		0:00-6:00	6:00-8:00	8:00-18:00	18:00-22:00	22:00-24:00
Occupancy	Weekdays	5%	30%	95%	30%	5%
	Weekends	5%	5%	30%	5%	5%
Equipment	Weekdays	15%	50%	95%	50%	15%
	Weekends	10%	10%	40%	10%	10%

2.2.2 PV modules

In this study, PV panels were installed on the roof of the building and the total rated installation capacity was 116.5 kW. The four-parameter equivalent diode model was used to generate the I-V curve of the PV module, as given by Eq. (1) [54].

$$I_{pv} = I_L - I_o \cdot \left[\exp\left(\frac{q}{\gamma k T_c} \left(V_{pv} + I_{pv} R_s \right) \right) - 1 \right] \quad (1)$$

where I_{pv} and V_{pv} are PV current (A) and voltage (V) respectively, q is electron charge

constant, k is Boltzmann constant (J/K), γ is the PV curve-fitting parameter, R_s is the module series resistance (Ω), I_L is the photocurrent (A) which is expressed by Eq. (2) and T_c is the module temperature (℃) which is calculated by Eq. (3).

$$I_L = I_{L,ref} \frac{G_T}{G_{T,ref}} \tag{2}$$

$$\frac{I_o}{I_{o,ref}} = \left(\frac{T_c}{T_{c,ref}} \right)^3 \tag{3}$$

where G_T is the solar radiation intensity incident on PV array (W/m^2), $G_{T,ref}$ is the solar radiation intensity under reference condition (1000 W/m^2), $I_{L,ref}$ is the module photocurrent under reference condition (A), $I_{o,ref}$ is the diode reverse saturation current under reference condition (A), $T_{c,ref}$ is the module temperature under reference conditions (25 ℃). According to Eq. (1) ~ (3), the I-V curve is associated with $I_{L,ref}$, $I_{o,ref}$, γ and R_s, which can be calculated using the algorithms given in Ref. [54].

A MPPT controller ensures the maximum power output of the PV system, as given by Eq. (4):

$$P_{pv} = \max(I_{pv} \cdot V_{pv}) \tag{4}$$

The installation tilt angle (α) was set as 34° which is considered the optimal tilt angle for PV installations in Changsha. The solar radiation intensity on the tilt plane is calculated by Eq. (5).

$$G_T = G_b R_b + G_d \left(\frac{1+\cos\alpha}{2} \right) + G\rho \left(\frac{1-\cos\alpha}{2} \right) \tag{5}$$

where G_b is the beam solar radiation intensity on the horizontal plane (W/m^2), R_b is the ratio of beam radiation of the inclined plane, G_d is the diffuse solar radiation intensity

on the horizontal plane (W/m^2), G is the global solar radiation intensity on the horizontal plane (W/m^2), ρ is the reflectance of the ground which is set as 0.2.

2.2.3 Batteries

The battery is modeled based on the state of charge (*SOC*), which is defined as the ratio of stored energy of the battery to its rated capacity, as given in Eq. (6).

$$SOC(t+1) = SOC(t) + \varepsilon \frac{P_{b,ch}(t)\Delta t \eta_{ch}}{E_b} - (1-\varepsilon)\frac{P_{b,dis}(t)\Delta t}{E_b \eta_{dis}} \tag{6}$$

where $P_{b,ch}$ is the charge power (kW), $P_{b,dis}$ is the discharge power (kW), η_{ch} is the charge efficiency (96%), η_{dis} is the discharge efficiency (96%), Δt is time step for calculation (Δt =1 h for this study), E_b is the battery rated capacity (kWh), ε is the binary number, 1 represents battery charge and 0 represents battery discharge..

There are two types of battery aging: calendar aging and cycle aging. Calendar aging is associated with *SOC* and temperature. In this study, temperature is assumed to be constant. The calendar aging at the t^{th} time step can be calculated by Eq. (7) [53].

$$\beta_{cal}(t) = 6.6148\times10^{-6} \times SOC(t) + 4.6404\times10^{-6} \tag{7}$$

Hence, the total calendar aging up to a given time (T) can be expressed by Eq. (8).

$$\beta_{cal}(T) = \sum_{t=1}^{T} \beta_{cal}(t) \tag{8}$$

The cycle aging at the t^{th} time step is given by Eq. (9).

$$\beta_{cyc}(t) = 0.5 \times \frac{|P_b(t)| \cdot \Delta t}{L_{cyc} \cdot E_b} \tag{9}$$

where P_b is the battery power (charge / discharge power), and L_{cyc} is the life cycle number of the battery. The cycle aging up to a given time (T) is calculated by Eq. (10)

[53, 55].

$$\beta_{cyc}(T) = 0.5 \times \frac{\sum_{t=1}^{T} |P_b(t)| \cdot \Delta t}{L_{cyc} \cdot E_b} \tag{10}$$

As a result, the total aging of the battery to a given time (T) is expressed by Eq. (11).

$$\beta_{total}(T) = \beta_{cal}(T) + \beta_{cyc}(T) \tag{11}$$

The battery state of health (SOH) is defined as the ratio of current usable capacity to the initial total battery capacity. Generally, when the battery aging reaches 1, the SOH is 0.8. Therefore, SOH is given by Eq. (12).

$$SOH(T) = 1 - 0.2 \times \beta_{total}(T) \tag{12}$$

The major parameters of the lithium-ion battery used in this study are listed in Table 3.

Table 3 Specifications of the lithium-ion battery used in this study

Parameters	Value
Charge/discharge efficiency	0.96
Life cycle number	4000
$SOC_{\min}$	0.2
$SOC_{\max}$	1
Maximum charge/discharge rate	0.2C

2.2.4 Electricity price

The time-of-use (TOU) tariff scheme was adopted in this study. According to the electricity market of Changsha, there are four electricity price periods in each day, defined as valley-price period (0:00-7:00, 22:00-24:00), flat-price period (7:00-8:00, 11:00-15:00), high-price period (8:00-11:00, 15:00-19:00) and peak-price period (19:00-22:00), as shown in Fig. 3. The surplus renewable electricity energy can be

exported to the grid with a feed-in-tariff (FiT) of 0.42 CNY/kWh.

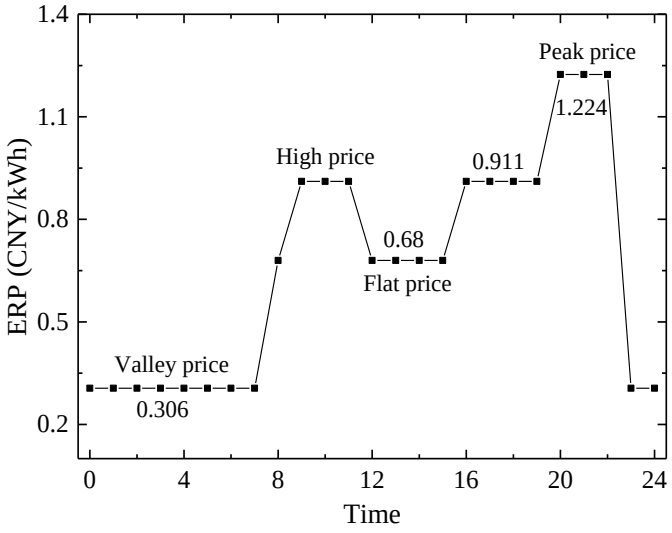

Fig. 3 Daily electricity retail price (ERP)

2.2.5 Techno-economic indicators

Self-consumption rate (*SCR*) and Self-sufficiency rate (*SSR*) are the most widely used indicators to assess the PV consumption and its contribution to the load demand, respectively. *SCR* focuses on the consumption of PV power generation, which is defined as the ratio of the PV power supplied to load and batteries to the total PV generation, as expressed by Eq. (13).

$$SCR = \frac{E_{p-d} + E_{p-b}}{E_{pv}} \tag{13}$$

where E_{p-d} is the total PV generation supplied directly to load (kWh), E_{p-b} is the total PV generation supplied to batteries (kWh), E_{pv} is the total PV generation (kWh).

SSR represents the ratio of the total PV generation that used directly by load and stored by batteries to the total load demand, which is given by Eq. (14).

$$SSR = \frac{E_{p-d} + E_{p-b}}{E_{de}} \tag{14}$$

where E_{de} is the total load demand (kWh).

In this study, the load cover ratio (*LCR*) is defined as the ratio of energy supplied by the PVB system to the load, which is given by Eq. (15).

$$LCR = \frac{E_{p-d} + E_{b-d}}{E_{de}} \tag{15}$$

where E_{b-d} is the total energy supplied by batteries to the load (kWh), which is the sum of total energy charged by PV and grid.

This study is conducted in terms of the annual operating performance of the PVB system. The total annual cost can be given by Eq. (16).

$$C_{total} = \sum_{t=1}^{8760} \left(C_{pv}^{t} + C_{b}^{t} + C_{g,im}^{t} - C_{g,ex}^{t} \right) \tag{16}$$

(1) C_{pv}^{t} is the cost derived from the PV system at the t^{th} time step, as calculated by:

$$C_{pv}^{t} = P_{pv}^{t} \cdot \Delta t \cdot x_{pv} \tag{17}$$

where P_{pv}^{t} is the PV power at the t^{th} time step (kWh), x_{pv} is the average cost of PV generation (CNY/kWh).

(2) C_{b}^{t} is the cost caused by battery degradation at the t^{th} time step:

$$C_{b}^{t} = \beta_{total}\left(t\right) \cdot x_{b} \cdot E_{b} \tag{18}$$

where $\beta_{total}\left(t\right)$ is the battery aging at the t^{th} time step, as given by Eq. (11), x_{b} is the unit capacity cost of the battery (CNY/kWh) including the initial investment and maintenance cost, as given by Eq. (19).

$$x_{b} = \left(x_{inv} + x_{mai} \right) \times E_{b} \tag{19}$$

where x_{inv} is the initial investment per unit capacity of the battery (CNY/kWh), x_{mai} is the maintenance cost per unit capacity of the battery (CNY/kWh), E_b is the battery capacity (kWh).

(3) $C_{g,im}^t$ is the cost for importing electricity from the utility grid at the t^{th} time step:

$$C_{g,im}^t = P_{g,im}^t \cdot \Delta t \cdot \mathrm{ERP}(t) \tag{20}$$

where $P_{g,im}^t$ is the power imported from the grid at the t^{th} time step (kW), ERP(t) is the electricity retail price at time step t.

(4) $C_{g,ex}^t$ is the revenue from exporting electricity to the grid at the t^{th} time step:

$$C_{g,ex}^t = P_{g,er}^t \cdot \Delta t \cdot \mathrm{FiT}(t) \tag{21}$$

where $P_{g,ex}^t$ is the power exported to the grid at the t^{th} time step (kW), and FiT is the feed-in-tariff (FiT) at time step t (CNY/kWh).

2.3 Operation strategies

Three operation strategies, including the DP-based strategy, the MSC strategy and the TOU strategy will be described in this part. The operational performance of the PVB system throughout the year will be simulated based on these strategies, with a temporal resolution of one hour.

2.3.1 DP-based strategy

The DP algorithm is a sequential optimization method for solving multistage optimization problems based on the optimality principle of the Bellman equation. Its basic idea is as follows: according to the optimal solution from the first stage to the t-1

stage and all possible solutions (the decision set) from the *t*-1 stage to the *t* stage, the optimal solution from the first stage to the *t* stage can be calculated based on the predetermined optimization objective. Then the final optimal solution of the whole process is obtained until the recursive exit is reached. DP emphasizes that whatever the initial state and decision are, the remaining decisions have to constitute the optimal strategy concerning the state of the first decision. As a result, the final optimization result of the problem is the accumulated optimum of the values selected in each step, which can ensure the global optimality.

In this study, the state of charge (*SOC*) of the battery is used as the control variable. At any time step *t*, all the possible *SOCs* of the battery form a series of uniformly discretized states ($SOC_t^1 \ldots SOC_t^{i(j)} \ldots SOC_t^n$). The decision set for any time step is given as {0.2:0.02:1}. The allowable state at the next time step (*t*+1) is dependent on the power constraints, and can be expressed by Eq. (22).

$$\max\left(SOC_{\min},\ SOC_t^i - \frac{P_b^{\lim}\Delta t}{E_b}\right) \le SOC_{t+1} \le \min\left(SOC_{\max},\ SOC_t^i + \frac{P_b^{\lim}\Delta t}{E_b}\right) \quad (22)$$

According to the principle of DP, the final *SOC* at a certain time step should be determined for achieving the minimum total operation cost from the first time step to the current time step. The operation cost in any time interval (*t*) can be calculated in two situations:

Situation I: $P_{de}^t - P_{pv}^t - P_b^t \ge 0$ (Importing electricity from the grid)

$$f_{t,1} = \left[P_{de}^t - P_{pv}^t - \left(SOC_{t-1} - SOC_t\right)\cdot E_b / \Delta t\right]\cdot \mathrm{ERP}(t) + C_{pv}^t + C_b^t \quad (23)$$

Situation I: $P_{de}^t - P_{pv}^t - P_b^t < 0$ (Exporting electricity to the grid)

$$f_{t,2}=\left[P_{de}^{t}-P_{pv}^{t}-\left(SOC_{t-1}-SOC_{t}\right)\cdot E_{b}/\Delta t\right]\cdot \mathrm{FiT}\left(t\right)+C_{pv}^{t}+C_{b}^{t} \tag{24}$$

where C_{pv}^{t} and C_{b}^{t} are the cost of the PV system and the cost caused by battery degradation, respectively, as given by Eq. (17) and Eq. (18).

The parameters in above models are subject to the following constraints:

(1) Power balance:

$$P_{de}^{t}=P_{pv}^{t}+P_{b}^{t}+P_{g}^{t} \tag{25}$$

where P_{de}^{t} is the demand electricity load (kW), P_{b}^{t} is the battery power (kW) ($P_{b}^{t}>0$ represents battery on discharge, $P_{b}^{t}<0$ represents battery on charge), and P_{g}^{t} is the electricity power exchanged with the grid ($P_{g}^{t}>0$ represents power imported from the grid, $P_{g}^{t}<0$ represents power exported to the grid) (kW).

(2) Battery charge/discharge rate limit:

$$\left|P_{b}^{t}\right|\le P_{b}^{\mathrm{lim}} \tag{26}$$

where P_{b}^{lim} is the charge/discharge rate limit of the battery, as given in Table 3 (0.2C).

(3) The state of charge (*SOC*) limit:

$$SOC_{\min}\le SOC_{t}\le SOC_{\max} \tag{27}$$

where $SOC_{\min}$ and $SOC_{\max}$ are the minimum and maximum *SOC* of the battery, respectively, as given in Table 3.

The flow chart of the DP method is shown in Fig. 4.

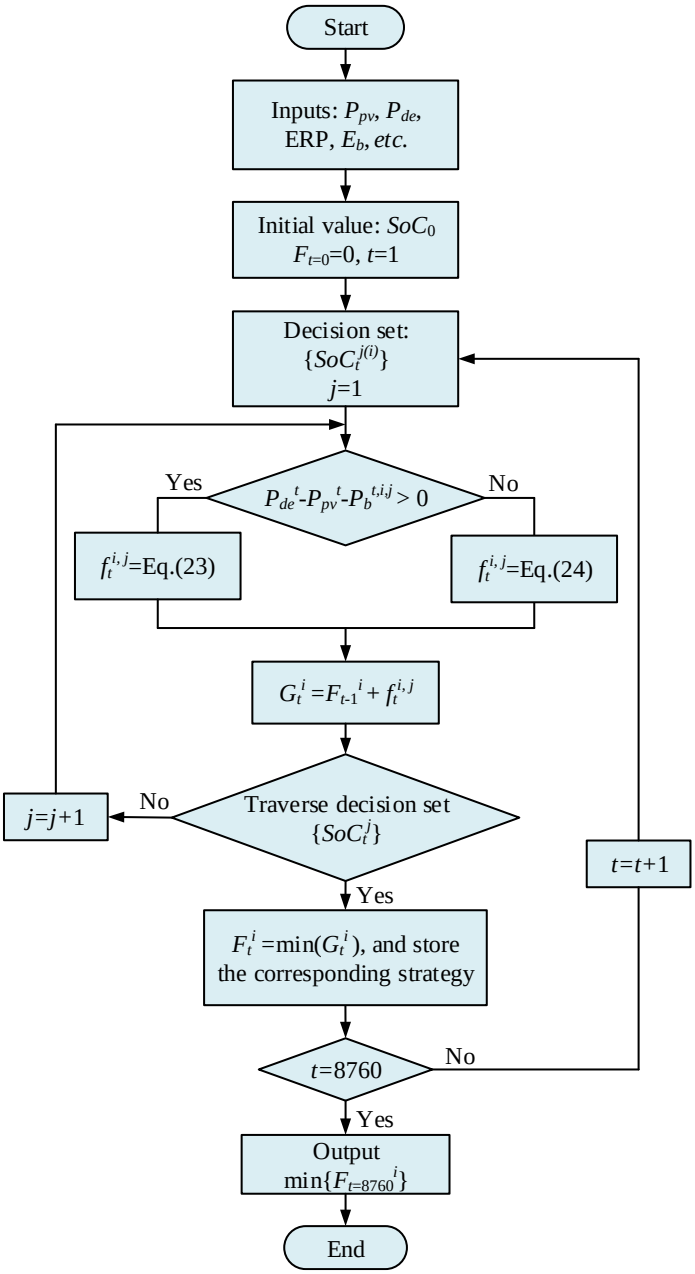

Fig. 4 Flow chart of the DP optimization strategy

2.3.2 Rule-based strategies

(1) MSC strategy

As mentioned previously, the MSC strategy is a basic and widely used energy management strategy for PV-integrated energy systems, which aims to use as much PV generated electricity for load demand and battery charge as possible. Its basic principle

is as follows: when PV power generation is larger than the load demand, surplus PV energy charges the battery first, and then excess energy is exported to the grid. When PV generation is less than the load demand, the battery discharges first to meet the load demand. If both the PV and battery cannot meet the load demand, electricity will be imported from the utility grid to cover the unmet load. A flow chart illustrating the MSC strategy is given in Fig. 5.

(2) TOU strategy

The TOU strategy is adopted to obtain economic benefit by taking advantage of the difference between the peak and valley electricity prices. The key point of the TOU strategy is to charge the battery during the valley price period using utility electricity, and then discharge electricity from battery to the load during high/peak periods. The flow chart of TOU strategy is given in Fig. 6.

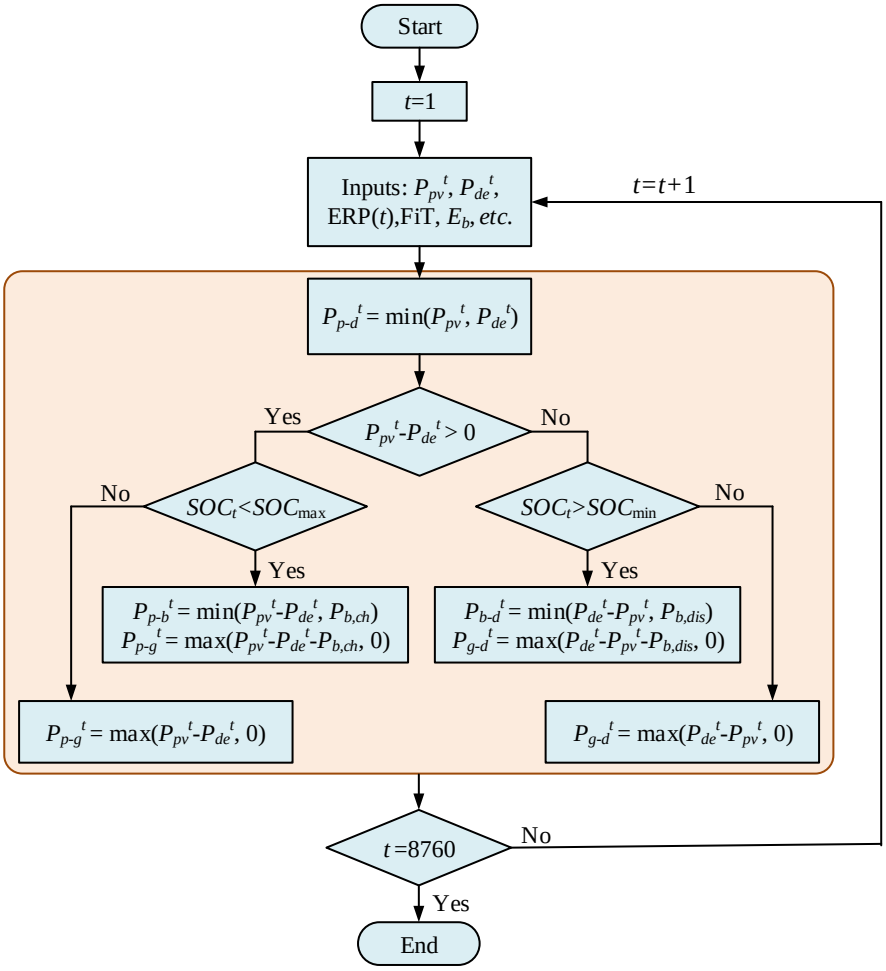

Fig. 5 Flow chart of the MSC operation strategy

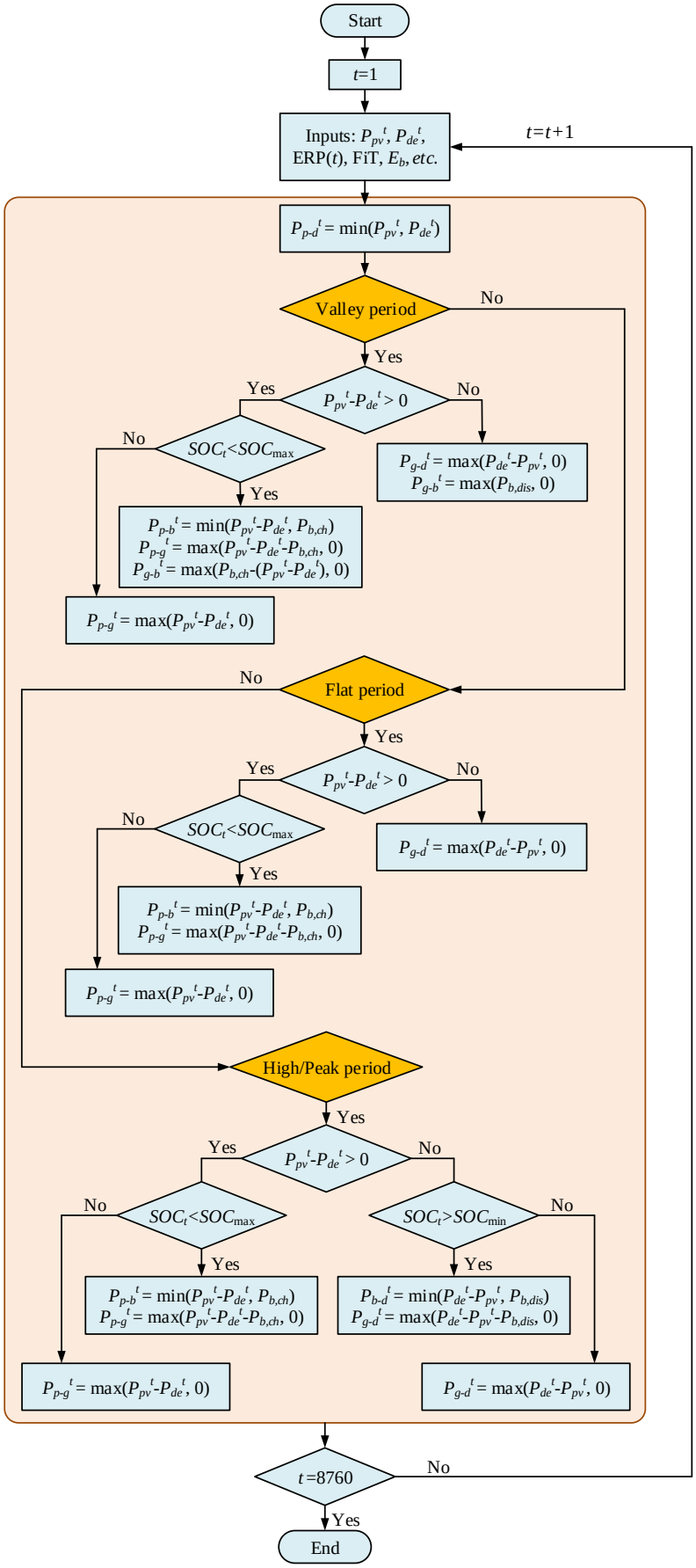

Fig. 6 Flow chart of the TOU operation strategy

3. Results and discussion

This section will give a detailed comparison of the grid-connected PVB system under the three operation strategies in terms of several important performance aspects, including the battery charge/discharge processes, techno-economic performance, energy distribution, battery aging and impact on the utility grid.

3.1 Scheduling results

3.1.1 Battery charge / discharge analysis

Fig. 7 shows the distribution of PV power and load demand, and the variation of battery *SOC* on two typical consecutive days under the three operation strategies. From the figure, it is seen that the PV generation and the load demand match very well in time, demonstrating that office buildings are very suitable for PV application. The charge/discharge processes of the three operation strategies are obviously different. As for the MSC strategy, the battery charge/discharge was only determined by the difference between the PV power and the load. When the PV power was larger than load, battery charges, otherwise it discharges. Moreover, the charge/discharge rate was proportional to the PV-load difference. As for the TOU strategy, except for charging when the PV power was larger than load, the battery was also charged at the maximum rate by the grid to be fully charged as soon as possible during the valley price period (23:00-1:00 the next day). During high or peak price periods, the battery discharged to meet the load which was not covered by the PV generation (9:00-11:00, 16:00-22:00). Unlike the two rule-based operation strategies (MSC and TOU), which usually charge

or discharge as fast as possible once the PV-load difference or the appropriate ERP periods occur, DP-based strategy controls flexibly the energy flow between the PV, battery and load to obtain the minimum cost for the whole year. In order to achieve as low cost as possible, the battery will also charge during the valley price period and discharge during the high and peak price periods, which is similar to the TOU strategy. However, the charge and discharge time of DP strategy is not the same as that of TOU strategy. For example, the battery started charging at 23:00 for the TOU strategy, while at 4:00 the next day for the DP strategy. This is because the DP strategy takes into account the coupling effects of all the hours behind, while the TOU strategy only considers the current time step. From Fig. 7, it is found that the charge/discharge rate of the DP strategy is different from those of the two rule-based strategies (MSC and TOU). This is because the charge/discharge rate is closely related to the total cost, as given by Eq. (23) and Eq. (24), which should be determined through economic optimization based on the whole year in the DP method, while for the rule-based strategies (MSC and TOU), it is determined only by the PV-load difference.

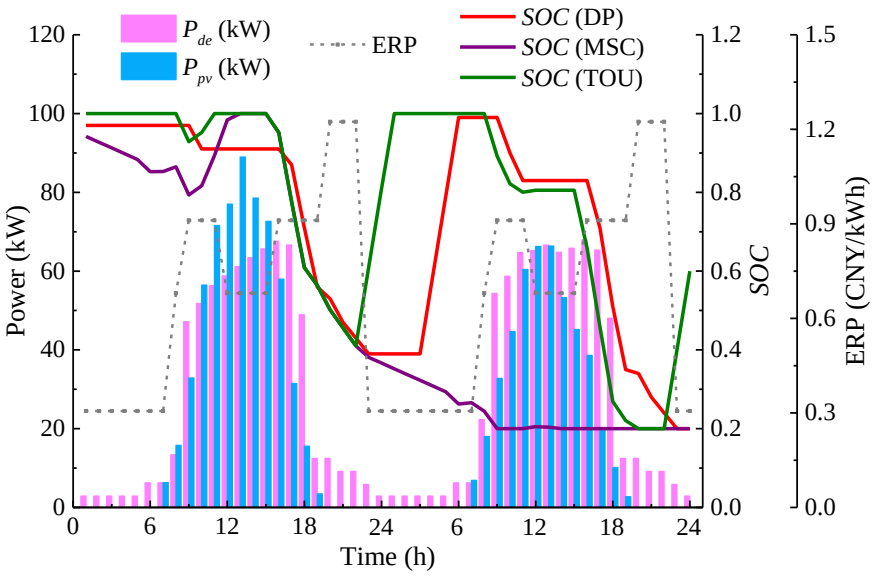

Fig. 7 Distribution of PV power and load demand and the variation of *SOC* over two typical consecutive days under the three operation strategies (P_{de} is the demand load, P_{pv} is the PV generation power)

More details about the energy dispatch are given in Fig. 8, which displays the power flow of the battery and the grid over the two typical consecutive days for the three operation strategies. Fig. 8 highlights another difference between the DP strategy and the two rule-based strategies. For example, at 10:00, the battery power and the grid power for DP strategy was 12 kW (battery on discharge) and -16.7 kW (exporting energy to the grid), respectively, while the PV power (56.5 kW) was larger than the load demand (51.8 kW). This indicates that the DP strategy will control flexibly the battery to discharge energy to the grid to obtain economic benefit through FiT even if the PV power is larger than the load demand. This effect is strikingly different from the two rule-based strategies (MSC and TOU) which only export surplus PV energy to the grid. Fig. 9 and Fig. 10 show the battery charge/discharge process determined by the DP strategy under conditions of different FiTs and different battery costs. It is evident from

the two figures that the charge/discharge process changed with different FiTs or battery costs. On the other hand, according to the principles of the two rule-based strategies (MSC and TOU) described in section 4.2, the charge/discharge processes will never be affected by the FiT and battery costs (x_b). Hence, it can be concluded that the DP strategy has greater flexibility than the rule-based strategies to adapt to various PV-load distributions and pricing mechanisms.

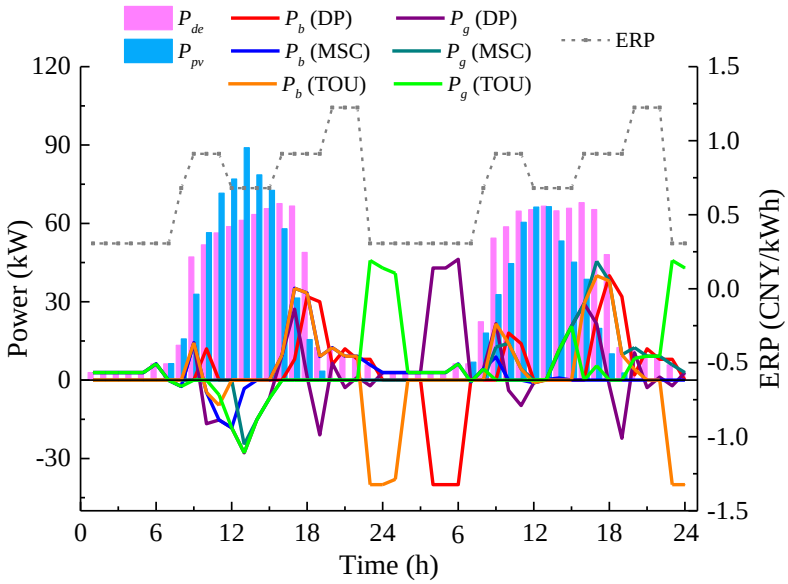

Fig. 8 Power flow over two typical consecutive days under the three operation strategies (P_{de} is the demand load, P_{pv} is the PV generation power, P_b is the battery charge/discharge power, P_g is the grid imported/exported power)

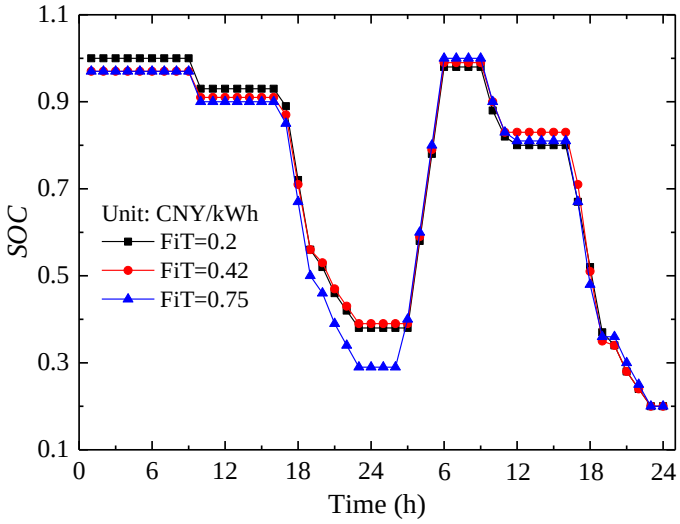

Fig. 9 Effects of FiT on charge/discharge process determined by the DP strategy

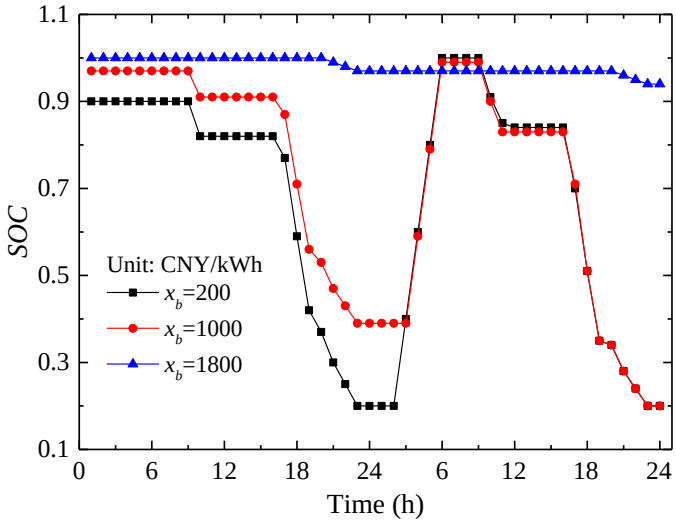

Fig. 10 Effects of battery cost (CNY/kWh) (x_b) on charge/discharge process determined by the DP strategy

3.1.2 Techno-economic performance

Fig. 11 depicts the total annual cost variation with battery size under the three operation strategies. It is clear that the total annual cost of the DP strategy was the smallest, and that of the MSC strategy was the largest. With the increase of battery size, the total annual costs for both the DP and MSC strategies increased, while that of the TOU strategy decreased. Moreover, the cost growth rate for the DP strategy was larger

than that of the MSC strategy. This indicates that the battery capacity is an important factor affecting the total operation cost of the PVB system, especially for the DP strategy. Fig. 12 and Fig. 13 show the effects of FiT and battery cost on the total annual cost under the three operation strategies, respectively. From Fig. 12, it is evident that the total annual costs for all the three strategies decreased with the increase of FiT. The total annual cost for the DP strategy dropped the most from 108919 CNY to -274771 CNY (negative value means it is profitable), which demonstrates that the economic performance of the DP strategy is more sensitive to FiT than the two rule-based strategies. Fig. 13 shows that the total annual costs for all the three strategies increased with battery cost increasing. When the battery cost increased to around 1600 CNY/kWh, the total annual cost for the TOU strategy was larger than that of the MSC strategy, indicating that the TOU strategy outperforms the MSC strategy in terms of economic performance only under the condition of relatively low battery costs.

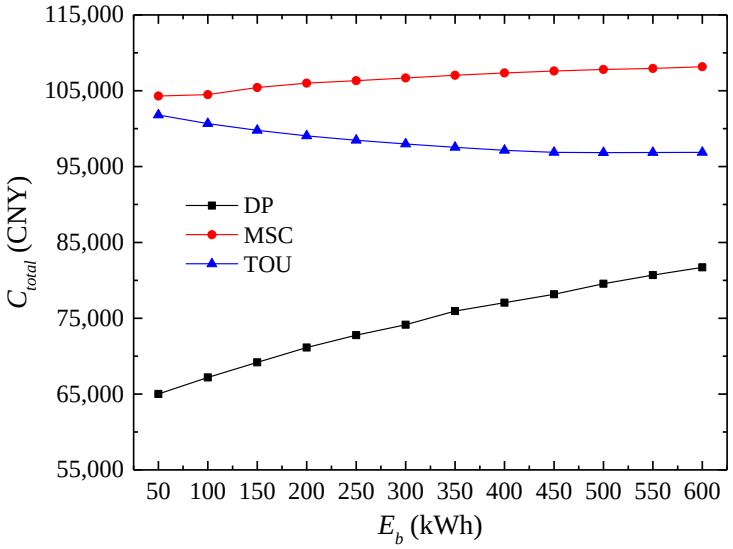

Fig. 11 Variation of the total annual cost (C_{total}) with battery size (E_b) under the three operation strategies

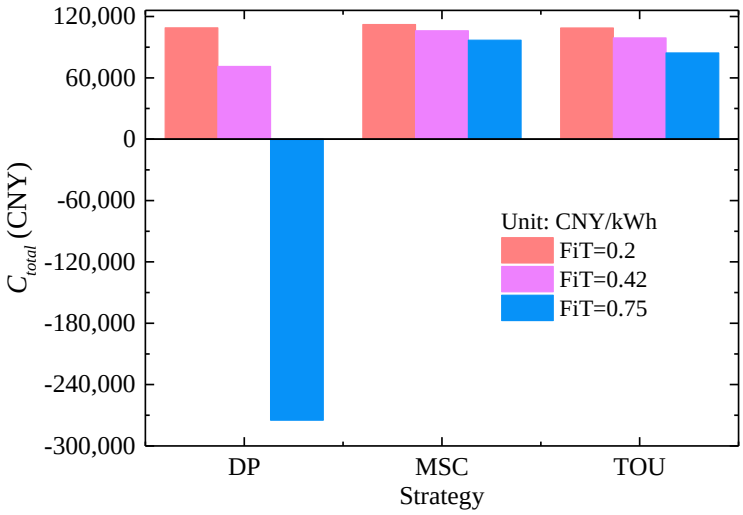

Fig. 12 Effects of feed-in-tariff (FiT) on the total annual cost (C_{total}) under the three operation strategies

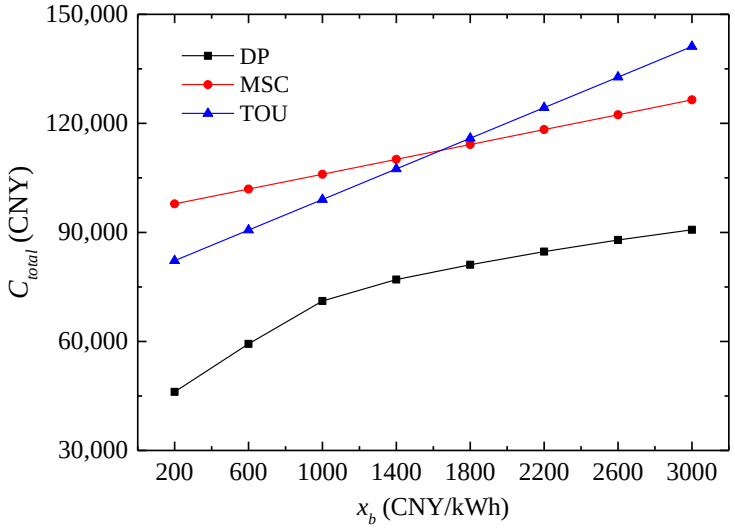

Fig. 13 Effects of battery cost (x_b) on the total annual cost (C_{total}) under the three operation strategies

Variations of the three technical indicators (*SCR*, *SSR*, *LCR*) for the three strategies are shown in Fig. 14 - 16. It is indicated in Fig. 14 and Fig. 15 that both *SCR* and *SSR* of the MSC strategy were much larger than those of the TOU strategy and DP strategy. They increased significantly with increasing battery size, while for TOU strategy and DP strategy, there was very little change. This is because the MSC strategy aims to use and store PV-generated energy in as timely a manner as possible, while the TOU

strategy and DP strategy determine the PV power uses (supplied to load, charging battery, or exported to grid) according to both PV-load distribution and electricity price. As Fig. 16 shows, the *LCR* of the TOU strategy was the largest, while that of the MSC strategy was the smallest, which indicates that the battery stores more energy imported from the grid under the TOU strategy. It is also found that the *LCR* remained almost constant as the battery size reached a certain value for both TOU and DP strategies, whereas for the MSC strategy, it increased continuously with increasing battery size. It can be expected from the increasing trend presented in Fig. 16 that the *LCR* of the MSC strategy will be larger than the *LCR* of the other two strategies (TOU and DP) as the battery size increases continuously. This is because larger battery size will store more surplus PV energy under the MSC strategy, while the energy distribution under the TOU and DP strategies is constrained by the objective of achieving economic benefit, which, consequently, limits the energy stored by the battery.

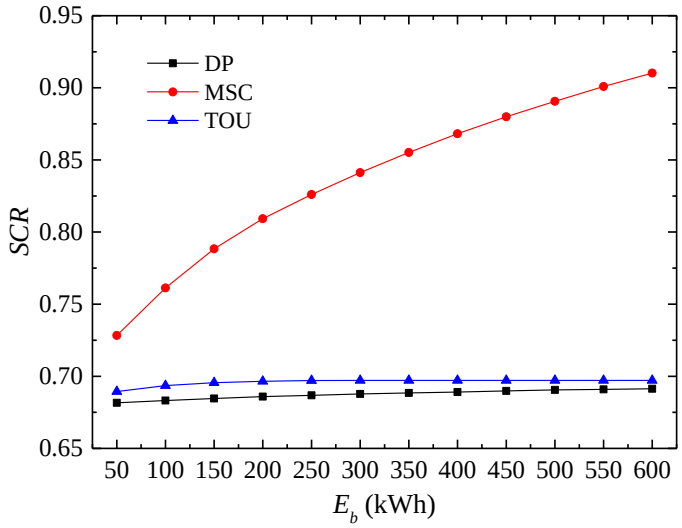

Fig. 14 Variation of self-consumption rate (*SCR*) with battery size (E_b) under the three operation strategies

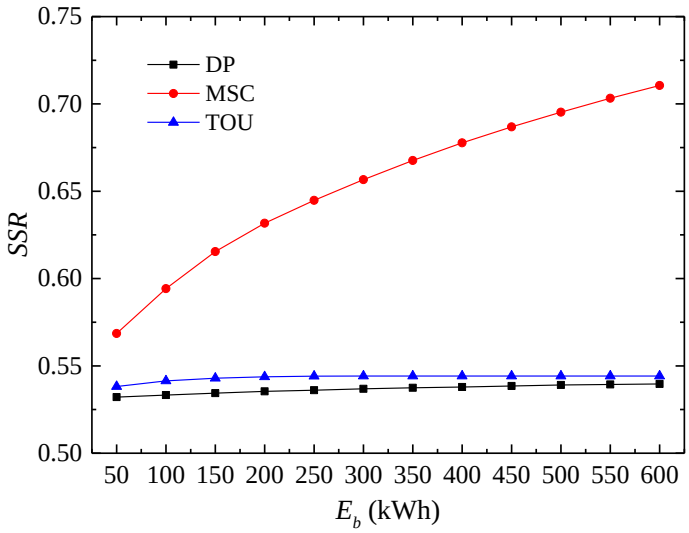

Fig. 15 Variation of self-sufficiency rate (*SSR*) with battery size (E_b) under the three operation strategies

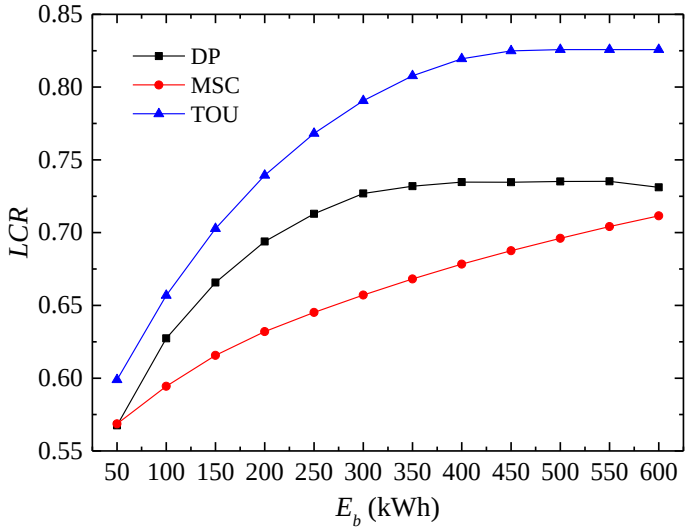

Fig. 16 Variation of load cover rate (*LCR*) with battery size (E_b) under the three operation strategies

3.2 Analysis of energy flow

Fig. 17 shows the breakdown of energy source (PV, battery, and grid) supplied to the load under the three operation strategies. It is clear that the PV generation supplied to the load was the same for each of the three strategies, while the battery-stored energy supplied to the load was the largest for the TOU strategy and the smallest for the MSC

strategy. This demonstrates that more energy provided by PV and the grid will be stored in the battery for the TOU strategy than the other two strategies, leading to higher *LCR*, as shown in Fig. 16. The uses of the total PV-generated energy, the total battery-stored energy and the total imported energy from grid under the three strategies are shown in Fig. 18, Fig. 19, and Fig. 20, respectively. Fig. 18 shows that the PV-generated energy that exceeds the load demand was more likely to be exported to the grid for both the DP and TOU strategies, while MSC strategy tended to use the excess PV energy to charge the battery. This is because the DP strategy and TOU strategy try to obtain economic benefit by exporting electricity to the grid with FiT. From Fig. 19, it is observed that the battery-stored energy for both the MSC and TOU strategies was all supplied to the load, while part of the battery-stored energy (7432.66 kWh) was exported to the grid for the DP strategy. This indicates again that the DP strategy will export flexibly the battery-stored energy to the grid to gain economic benefit through FiT, as discussed in section 3.1. The energy imported from the grid was all supplied to load for the MSC strategy, as shown in Fig. 20. This is because the MSC strategy only uses the excess PV energy to charge the battery. As for the DP strategy and TOU strategy, a significant portion of the imported energy from the grid was used to charge the battery —37021 kWh for DP strategy and 36623 kWh for TOU strategy. This is because both the DP and TOU strategies tend to charge the battery during valley price times and discharge during high/peak price times to obtain economic benefit through the valley-peak (high) price difference.

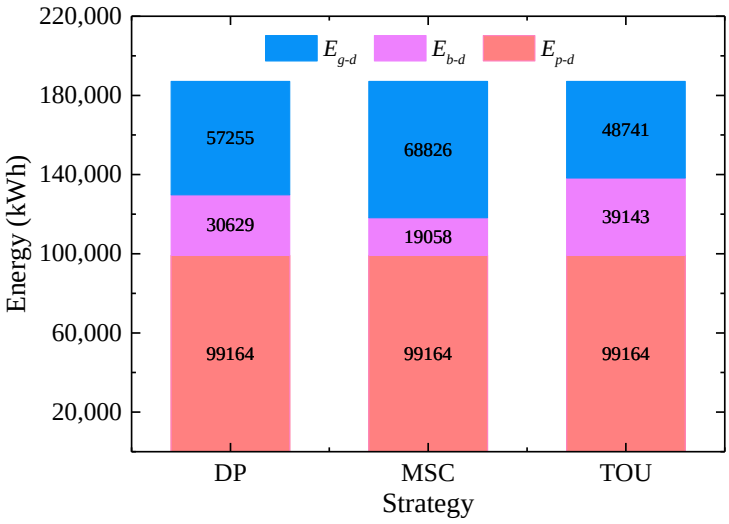

Fig. 17 Breakdown of energy source supplied to load under the three operation strategies

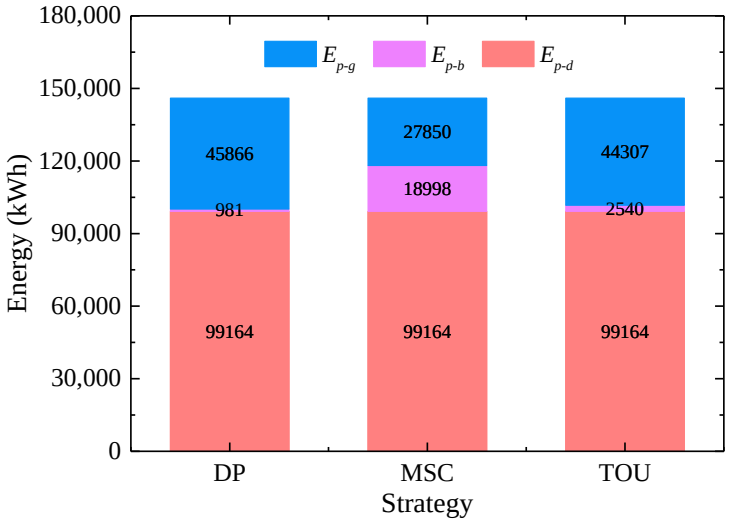

Fig. 18 Uses of total PV-generated energy under the three operation strategies

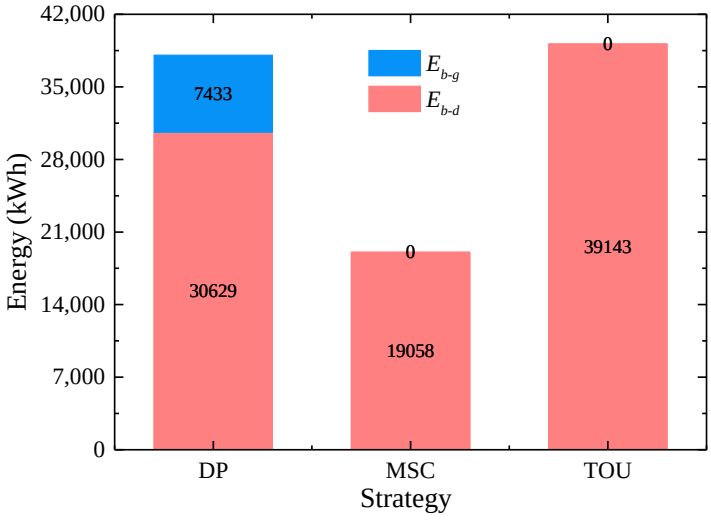

Fig. 19 Uses of total battery-stored energy under the three operation strategies

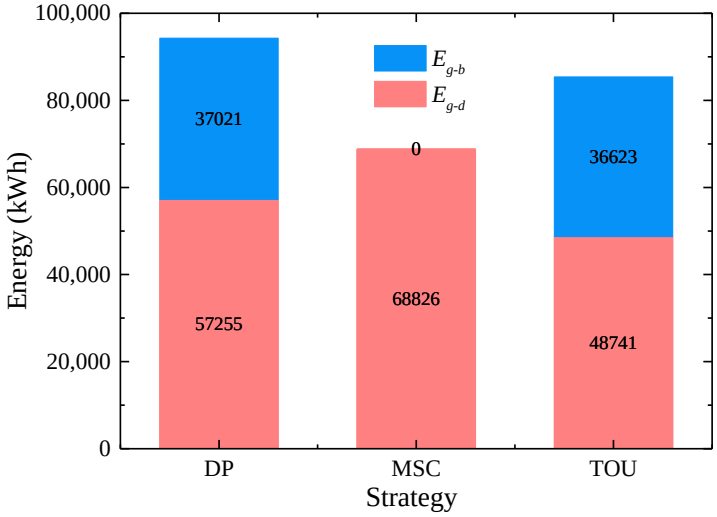

Fig. 20 Uses of total energy imported from grid under the three operation strategies

3.3 Battery aging and impact on the utility grid

3.3.1 Battery aging

Fig. 21 shows the battery aging and *SOH* under the three operation strategies. It is found that both the calendar aging and cycle aging of the MSC strategy were the smallest and those of the DP strategy were slightly smaller than those of the TOU strategy. The *SOH* for the DP strategy, the MSC strategy, and the TOU strategy was 0.969, 0.979, and 0.967, respectively. This demonstrates that the TOU strategy causes the largest reduction of battery health, slightly larger than that of the DP strategy, and the MSC strategy has the least impact on battery health. The reasons for this effect are displayed in Fig. 22 and Fig. 23, which show the total annual discharge energy and discharge hours, and the distribution of *SOC* under the three strategies, respectively. It is clear in Fig. 22 that the TOU strategy has the largest total discharge energy (39143 kWh) and the shortest discharge hours (2296 h), while the MSC strategy has the

smallest total discharge energy (19058 kWh) and the longest discharge hours (2814 h), which means that the TOU strategy has the largest discharge depth and the MSC strategy has the smallest. As a result, the TOU strategy will cause the most severe cycle aging of the battery and the MSC strategy causes the least. From Fig. 23, it is found that the average *SOC* (the small box) for the TOU strategy was the largest (0.8) and that for the MSC was the smallest (0.46). Moreover, the *SOC* at the median line for the DP strategy, the MSC strategy and the TOU strategy was about 0.63, 0.2 and 1, respectively, which means that for most of the time the *SOC* is at a high value for the TOU strategy and a small value for the MSC strategy. Consequently, according to Eq. (7), the TOU strategy causes the most significant calendar aging of the battery, and the MSC strategy causes the least, as presented in Fig. 21. From Fig. 22 and Fig. 23, it can also be found that both the total discharge energy and the average *SOC* for DP and TOU strategies were close, which means the difference of battery aging caused by these two strategies will not be obvious, as given in Fig. 21.

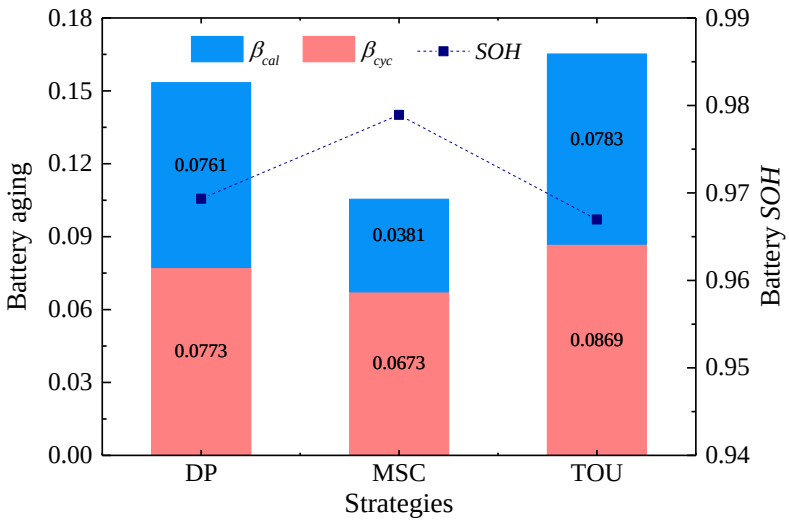

Fig. 21 Battery aging and *SOH* under the three operation strategies

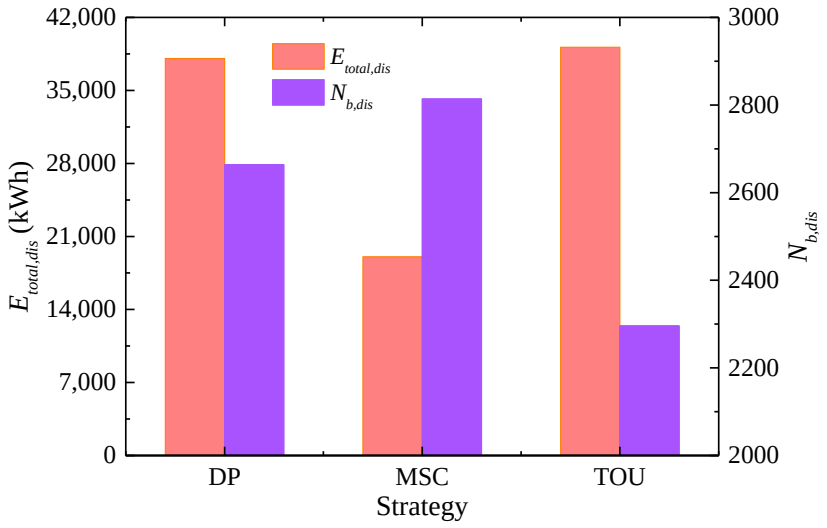

Fig. 22 Total annual discharge energy and discharge hours of the battery under the three operation strategies

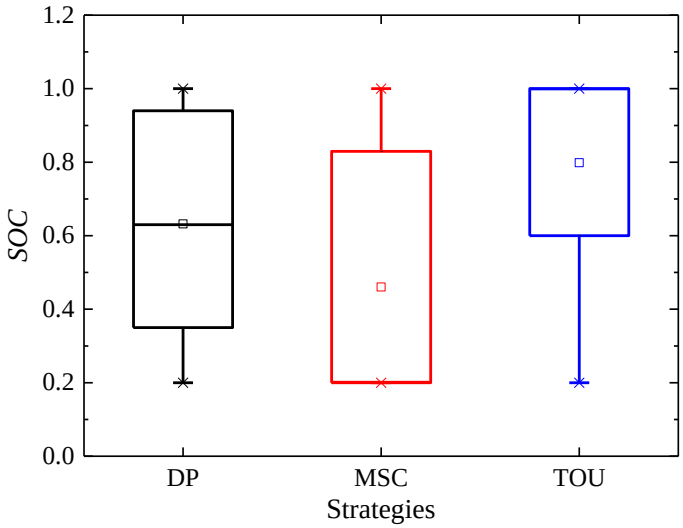

Fig. 23 Distribution of *SOC* under the three operation strategies

3.3.2 Impact on the utility grid

Fig. 24 shows the annual total energy imported from and exported to the grid under the three operation strategies. Both the total imported energy and exported energy for the MSC strategy were less than those for the DP strategy and TOU strategy, which have a similar imported and exported energy. This is because both the DP strategy and TOU strategy tend to import energy from the grid during the valley price periods and

export energy to the grid during the higher price periods. In order to analyze the impact of each operation strategy on the grid, the total imported energy and exported energy in each electricity price period are presented in Fig. 25. It is clear from Fig. 25(a) that the imported energy for both the DP and TOU strategies were the largest in valley price period and decreased significantly in the higher price periods (high and peak price), whereas the largest imported energy for the MSC strategy occurred in high-price period. This reveals that the MSC strategy put much more burden on the grid compared to both the DP and TOU strategies. From Fig. 25(b), it is easily observed that the exported energy of both the DP and TOU strategies was larger than that of the MSC strategy, which is due to the DP and TOU strategies trying to export energy to grid to obtain economic benefit through FiT. The larger exported energy during high and peak periods is good for reducing the power supply burden of the grid, demonstrating that the DP strategy and TOU strategy have the advantage of achieving grid-relief than the MSC strategy. It is also found from Fig. 25(a)-(b) that the imported energy of the DP strategy was much less than that of the TOU strategy during the peak-price hours, while the exported energy of the DP strategy was more than that of the TOU strategy in the high and peak price periods. This indicates that the DP strategy has the biggest advantage of reducing burden on the utility grid among the three strategies.

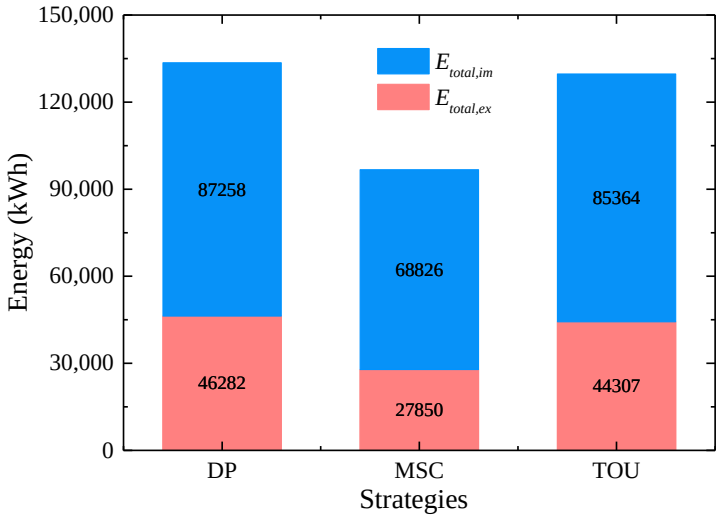

Fig. 24 Annual total energy imported from and exported to the utility grid under the three operation strategies

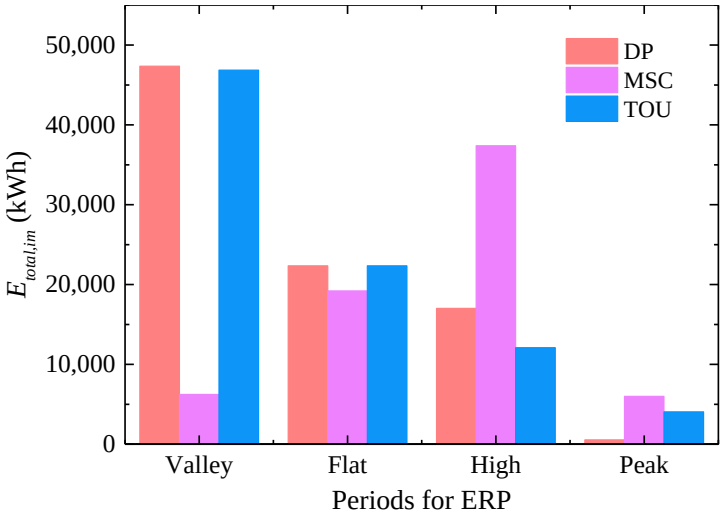

(a) Imported energy in each ERP period

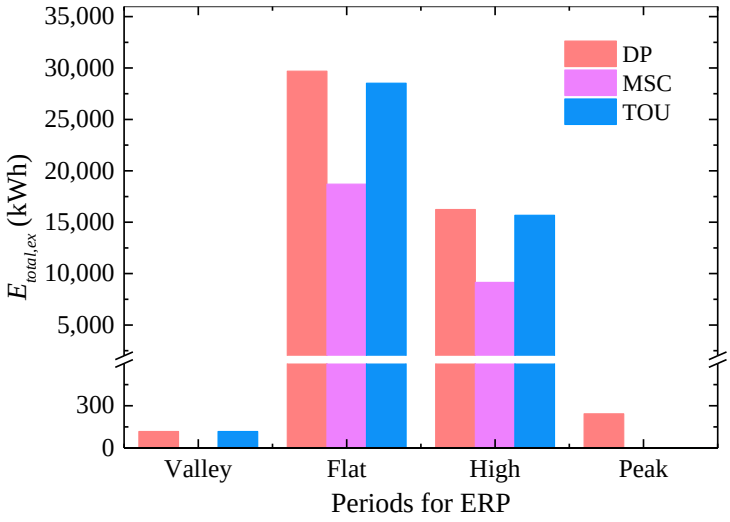

(b) Exported energy in each ERP period

Fig. 25 Annual total energy imported from and exported to the utility grid in each ERP period under the three operation strategies (valley period: 0:00-7:00, 22:00-24:00; flat period: 7:00-8:00, 11:00-15:00; high period: 8:00-11:00, 15:00-19:00, peak period: 19:00-22:00)

4. Conclusions

In this study, three operation strategies, including the DP based strategy, the MSC strategy and the TOU strategy, were compared comprehensively for the PVB system used in an office building. Several important performance aspects, such as battery charge/discharge performance, techno-economic performance, energy flow distribution, battery aging and impacts on the utility grid, were discussed and evaluated. It was found that the three strategies differ greatly in each aspect of performance. The findings can provide a guidance for stakeholders and engineers to optimize the management of grid-connected PVB systems. Several conclusions can be drawn as follows:

(1) Constrained by the rules of the strategy itself, the MSC strategy and TOU strategy control the battery charge/discharge process just based on the current PV-load difference and the electricity price. In contrast, the DP strategy determines the charge/discharge process considering the coupling effects of all stages and controls flexibly the power flow to obtain the minimum cost. The DP strategy has greater flexibility than the two rule-based strategies (MSC and TOU) to adapt to different PV-load distributions and electricity pricing mechanisms.

(2) The DP strategy has the best economic performance among the three strategies. The TOU strategy only outperforms the MSC strategy in economic performance under

the condition of relatively low battery cost (<1600 CNY/kWh). Both the *SCR* and *SSR* of the MSC strategy are much larger than those of the TOU strategy and DP strategy. The *LCR* of the MSC strategy increases significantly with increasing battery capacity, while that of the TOU and DP strategies remains almost constant as battery capacity reaches around 450 kWh.

(3) The DP strategy exports appropriately the battery-stored energy to the grid to gain economic benefit through FiT, even if the PV generation is larger than the load demand. The TOU strategy causes the most significant battery aging while the MSC strategy causes the least. The battery aging caused by the DP strategy is slightly smaller than that caused by the TOU strategy due to their close total charge energy and annual average *SOC*. The DP strategy has the biggest advantage of reducing burden on the utility grid and the MSC strategy puts the greatest burden on the utility grid.

The proper energy dispatch strategy for PVB systems in engineering practice should be determined in accordance with specific requirements and in-depth consideration of the significance of each aspect of performance. The timing match of PV generation and load demand is an important factor affecting the battery capacity and the scheduling strategy of the system. Therefore, in future work, the coupling optimization of sizing and scheduling of PVB systems under different timing match conditions of PV generation and load demand will be investigated.

5. Acknowledgements

This work was supported by the China Postdoctoral Science Foundation

(2020M682559) and the Science and Technology Innovation Program of Hunan Province (2020RC2017, 2020RC5003, 2017XK2015).

References

[1] Li D.H.W, Pan WY, Lam JC. A comparison of global bioclimates in the 20th and 21st centuries and building energy consumption implications. Energy and Environment 2014; 75: 236-249.

[2] Costa A, Keane MM, Torrens JI, Corry E. Building operation and energy performance: monitoring, analysis and optimization toolkit. Applied Energy 2013;101: 310-316.

[3] Hu S, Yan D, Guo SY, Cui Y, Dong B. A survey on energy consumption and energy usage behavior of households and residential building in urban China. Energy and Buildings. 2017; 148: 366-378.

[4] Cabeza LF, Chafer M. Technological options and strategies towards zero energy buildings contributing to climate change mitigation: A systematic review. Energy and Buildings 2020; 219: 110009.

[5] Lin YL, Zhong SL, Yang E, Hao XL, Li CQ. Towards zero-energy buildings in China: A systematic literature review. Journal of Cleaner Production 2020; 276: 123297.

[6] Wang R, Feng W, Wang L, Lu SL. A comprehensive evaluation of zero energy buildings in cold regions: Actual performance and key technologies of cases from China, the US, and the European Union. Energy 2021; 215: 118992.

[7] Sobhani H, Shahmoradi F, Sajadi B. Optimization of the renewable energy system for nearly zero energy buildings: A future-oriented approach. 2020; 224: 113370.

[8] REN21. Renewables 2020 global status report. 2020. https://ren21.net/gsr-2020/

[9] Yan JY, Yang Y, Campana, PE, He JJ. City-level analysis of subsidy-free solar photovoltaic electricity price, profits and grid parity in China. Nature Energy 2019; 4: 709-717.

[10] Peng JQ, Curcija D, Thanachareonkit A, Lee E, Goudey H, Selkowitz S. Study on the overall energy performance of a novel c-Si based semitransparent solar photovoltaic window. Applied Energy 2019; 242: 854-872.

[11] Peng JQ, Yan JY, Zhai ZQ, Markides CN, Taylor RA. Solar energy integration in buildings. Applied Energy 2020; 264: 114740.

[12] IRENA. Future of Solar Photovoltaic: Deployment, investment, technology, grid integration and socio-economic aspects. International Renewable Energy Agency, Abu Dhabi, 2019.

[13] Zhang Y, Lundblad A, Campana PE, Yan JY. Employing battery storage to increase photovoltaic self-sufficiency in a residential building of Sweden. Energy Procedia 2016; 88: 455-461.

[14] Schram WL, Lampropoulos I, Sark W. Photovoltaic systems coupled with batteries that are optimally sized for household self-consumption: Assessment of peak shaving potential. Applied Energy 2018; 223: 69-81.

[15] Azuatalam D, Paridari K, Förstl M, Chapman AC, Verbič G. Energy management

of small-scale PV-battery systems: A systematic review considering practical implementation, computational requirements, quality of input data and battery degradation. Renewable and Sustainable Energy Reviews 2019; 112: 555-570.

[16] Chakir A, Tabaa M, Moutaouakkil F, Medromi H, Julien-Salame M, Dandache A, Alami K. Optimal energy management for a grid connected PV-battery system. Energy Reports 2020; 6: 218-231.

[17] Zhang YJ, Ma T, Campana PE, Yamaguchi Y, Dai YJ. A techno-economic sizing method for grid-connected household photovoltaic battery systems. Applied Energy 2020; 269: 115106.

[18] Braun M, Büdenbender K, Magnor D, Jossen A. Photovoltaic self-consumption in Germany – using lithium-ion storage to increase self-consumed photovoltaic energy. 2009. https://www.researchgate.net/publication/43248782

[19] Talavera DL, Mo-RFJ, G J-C, C R-C. A new approach to sizing the photovoltaic generator in self-consumption systems based on cost–competitiveness, maximizing direct self-consumption. Renewable Energy 2019; 130: 1021-1035.

[20] Hernandez JC, Sanchez-Sutil F, Munoz-Rodríguez FJ. Design criteria for the optimal sizing of a hybrid energy storage system in PV household-prosumers to maximize self-consumption and self-sufficiency. Energy 2019; 186: 115827.

[21] Luthander R, Widén J, Nilsson D, Palm J. Photovoltaic self-consumption in buildings: A review. Applied Energy 2015; 142: 80-94.

[22] Sharma V, H.Haque M, Asis SM. Energy cost minimization for net zero energy

homes through optimal sizing of battery storage system. Renewable Energy 2019; 141: 278-286.

[23] Nyholm E, Goop J, Odenberger M, Johnsson F. Solar photovoltaic-battery systems in Swedish households – self-consumption and self-sufficiency. Applied Energy 2016; 183: 148-159.

[24] Angenendt G, Zurmühlen S, Axelsen H, Sauer DU. Comparison of different operation strategies for PV battery home storage systems including forecast-based operation strategies. Applied Energy 2018; 229: 884-899.

[25] Dusonchet L, Telaretti E. Comparative economic analysis of support policies for solar PV in the most representative EU countries. Renewable and Sustainable Energy Reviews. 2015; 42: 986-998.

[26] Flath CM. An optimization approach for the design of time-of-use rates. 39th Annual Conference of Industrial Electronics Society, Vienna, Austria, 2013; pp. 4727-4732.

[27] Li R, Wang Z, Gu C, Li F, Wu H. A novel time-of-use tariff design based on Gaussian Mixture Model. Applied Energy 2016; 162: 1530-1536.

[28] Darghouth NR, Wiser RH, Barbose G. Customer economics of residential photovoltaic systems: sensitivities to changes in wholesale market design and rate structures, Renewable and Sustainable Energy Review 2016; 54: 1459-1469.

[29] Gitizadeh M, Fakharzadegan H. Battery capacity determination with respect to optimized energy dispatch schedule in grid-connected photovoltaic (PV) systems.

Energy 2014; 65: 665-674.

[30] Hassan AS, Cipcigan L, Jenkins N. Optimal battery storage operation for PV systems with tariff incentives. Applied Energy 2017; 203: 422-441.

[31] Ratnam EL, Weller SR, Kellett CM. An optimization-based approach to scheduling residential battery storage with solar PV: assessing customer benefit. Renewable Energy 2015; 75: 123-134.

[32] Zhang SR, Tang YL. Optimal schedule of grid-connected residential PV generation systems with battery storages under time-of-use and step tariffs. Journal of Energy Storage 2019; 23: 175-182.

[33] Liu J, Chen X, Yang HX, Li YT. Energy storage and management system design optimization for a photovoltaic integrated low-energy building. Energy 2020; 190: 116424.

[34] Liu J, Wang M, Peng JQ, Chen X, Cao SL, Yang HX. Techno-economic design optimization of hybrid renewable energy applications for high-rise residential buildings. Energy Conversion and Management 2020; 213: 112868.

[35] Abdmouleh Z, Gastli A, Ben-Brahim L, Haouari M, Al-Emadi NA. Review of optimization techniques applied for the integration of distributed generation from renewable energy sources. Renewable Energy 2017; 113: 266-280.

[36] Ghorbani N, Kasaeian A, Toopshekan A, Bahrami L, Maghami A. Optimizing a hybrid wind-PV-battery system using GA-PSO and MOPSO for reducing cost and increasing reliability. Energy 2018; 154: 581-591.

[37] Sharafi M, EL Mekkawi TY. Multi-objective optimal design of hybrid renewable energy systems using PSO-simulation based approach, Renewable Energy 2014; 68: 67-79.

[38] Yousefi H, Ghdusinejad MH, Noorollahi Y. GA/AHP-based optimal design of a hybrid CCHP system considering economy, energy and emission, Energy and Buildings 2017; 138: 309-317.

[39] Liu J, Chen X, Yang HX, Shan K. Hybrid renewable energy applications in zero-energy buildings and communities integrating battery and hydrogen vehicle storage. Applied Energy 2021; 290: 116733.

[40] Sahoo U, Kumar R, Singh SK, Tripathi AK. Energy, exergy, economic analysis and optimization of polygeneration hybrid solar-biomass system. Applied Thermal Engineering 2018; 145: 685-692.

[41] Nottrott A, Kleissl J, Washom B. Energy dispatch schedule optimization and cost benefit analysis for grid-connected, photovoltaic-battery storage systems. Renewable Energy 2013; 55: 230-240.

[42] Georgiou GS, Christodoulides P, Kalogirou SA. Optimizing the energy storage schedule of a battery in a PV grid-connected nZEB using linear programming. Energy 2020; 208: 118177.

[43] Yang F, Xia XH. Techno-economic and environmental optimization of a household photovoltaic-battery hybrid power system within demand side management. Renewable Energy 2017; 108: 132-143.

[44] Javadi MS, Gough M, Lotfi M, Nezhad AE, F. Santos S, P.S. Catalao J. Optimal self-scheduling of home energy management system in the presence of photovoltaic power generation and batteries. Energy 2020; 210: 118568.

[45] Chen XP, Hewitt N, Li ZT, Wu QM, Yuan X, Roskilly T. Dynamic programming for optimal operation of a biofuel micro CHP-HES system. Applied Energy 2017; 208: 132-141.

[46] Bahlawan H, Morini M, Pinelli M, Spina PR. Dynamic programming based methodology for the optimization of the sizing and operation of hybrid energy plants. Applied Thermal Engineering 2019; 160: 113967.

[47] Bernasconi G, Brofferio S, Cristaldi L. Cash flow prediction optimization using dynamic programming for a residential photovoltaic system with storage battery. Solar Energy 2019; 186: 233-246.

[48] Bhoi SK, Nayak MR. Optimal scheduling of battery storage with grid tied PV systems for trade-off between consumer energy cost and storage health. 2020; 79: 103274.

[49] Ming B, Liu P, Cheng L, Zhou Y, Wang X. Optimal daily generation scheduling of large hydro-photovoltaic hybrid power plants. 2018; 171: 528-540.

[50] Mahmoudimehr J, Sebghati P. A novel multi-objective dynamic programming optimization method: Performance management of a solar thermal power plant as a case study. Energy 2019; 168: 796-814.

[53] R.E. Bellman, Dynamic Programming, Princeton University Press, 1957.

[52] Zhang Y, Lundblad A, Campana PE, Benavente F, Yan JY. Battery sizing and rule-based operation of grid-connected photovoltaic-battery system: A case study in Sweden. Energy Conversion and Management 2017; 133: 249-263.

[53] Mulleriyawage UGK, Shen WX. Optimally sizing of battery energy storage capacity by operational optimization of residential PV-Battery systems: An Australian household case study. Renewable Energy 2020; 160: 852-864.

[54] Department of Energy. Energyplus Engineering Reference (Version 9.3).

[55] Hesse H, Martins R, Musilek P, Naumann M, Truong C, Jossen AJE. Economic optimization of component sizing for residential battery storage systems. Energies 2017; 10: 835-853.